Journal of Alloys and Compounds 505 (2010) 362–366

Contents lists available at ScienceDirect

Journal of Alloys and Compounds

journal homepage: www.elsevier.com/locate/jallcom

The structure and optical properties of ZnO nanocrystals dependence on Co-doping levels

Sha Wang, Ping Li*, Hui Liu, Jibiao Li, Yu Wei*

Provincial Key Laboratory of Inorganic Nanomaterials, School of Chemistry and Materials Science, Hebei Normal University, Yuhua Road 113#, Shijiazhuang 050016, China

ARTICLE INFO

Article history:
Received 5 January 2010
Received in revised form 8 May 2010
Accepted 14 May 2010
Available online 19 June 2010

Keywords:
Semiconductors
Nanostructured materials
Precipitation
Optical property

ABSTRACT

Pure and Co-doped ZnO (Co:ZnO) nanocrystals with different doping levels were synthesized via a coprecipitation process. The structure and morphology of the as-prepared samples were characterized by XRD, EDS, XPS and FESEM. Results show that cobalt ions, in the oxidation state of Co^{2+}, replace Zn^{2+} ions into the ZnO lattice without changing its wurtzite structure. The dopant content varies from 0.35 to 2.94% depending on Co-doping levels. The particles have a nearly spherical morphology with dimensions of 80–150 nm for pure ZnO and 50–120 nm for Co:ZnO. The optical properties of the samples were studied by UV–vis absorption and PL spectra. The band gap of Co:ZnO nanocrystals decreases with the increasing dopant content, resulting in red shifts of the wavelength in UV absorption and PL emissions.

1. Introduction

ZnO is a multifunctional inorganic semiconductor material with a wide band gap (3.37 eV) and large exciton binding energy (60 meV) [1,2]. It has emerged as one of the most promising oxide materials because of its numerous industrial applications in many fields. ZnO has been extensively used in medicines, pigments, catalysts, ceramics, rubber additives, and so on [3–5]. Nowadays, ZnO has been investigated as an excellent optoelectronic material for fabricating solar cells, electrodes, sensors, transparent UV-protection films and UV light emitting devices [6–8]. As is reported recently, doping in ZnO with selective elements offers an effective method to adjust its electrical, optical, and magnetic properties [9–11], which is crucial for its practical applications. Transition metal elements, such as cobalt, are rich in electron states. Appropriate amount of Co-doping can tune both optical and magnetic properties without changing the crystal structure of ZnO. A number of research groups are dedicated to the preparation of Co-doped ZnO (Co:ZnO) nanocrystals [12–17]. However, a lot of work done focused on the magnetic properties of Co:ZnO, only a few studies on the optical properties.

Many techniques can be used to synthesize ZnO nanocrystals, such as chemical vapor deposition (CVD) [18,19], thermal evaporation [20,21], precipitation method [22] and various hydrothermal methods [23–26]. Among them, the coprecipitation method has attracted our interests in the synthesis of Co:ZnO nanocrystals. Because the reagents are mixed at molecular level in this process, Co ions can be easily incorporated into ZnO and replace Zn ions in the lattice. Herein, our researches focus on the preparation of pure ZnO and Co:ZnO nanocrystals via the coprecipitation method. Using $ZnCl_2$, NaOH and $CoCl_2$ as raw materials, well-crystalline pure ZnO and Co:ZnO nanocrystals were successfully synthesized and followed by a variety of characterization. The influences of Co-doping on the microstructure and morphology of ZnO were investigated in detail. In particular, the optical properties of the samples, which were received from UV–vis absorption and PL spectra, exhibited significant diversification after Co-doping.

2. Experimental

2.1. Preparation of pure ZnO and Co:ZnO nanocrystals

Zinc chloride ($ZnCl_2$), cobalt chloride ($CoCl_2$) and sodium hydroxide (NaOH) in these experiments were of analytical grade and used without further purification. $ZnCl_2$, $CoCl_2$ and NaOH were dissolved at room temperature in deionized water to obtain 1.0, 0.1 and 2.0 M, respectively, standard solutions prior to the synthetic experiments. Pure ZnO and Co:ZnO nanocrystals were prepared by a coprecipitation method described as follows: 20 ml of the $ZnCl_2$ solution was added dropwise to 17 ml of the NaOH solution with an additional 43 ml of deionized water under vigorous stirring at 25 °C. Different volumes (0, 2, 6, 10, 16 and 20 ml) of the $CoCl_2$ solution were then added dropwise to the above mixture, according to the required Co-doping levels. The resulting precipitate was filtered, thoroughly washed and then dried in air at ambient temperature. Finally the precipitate was calcined in a Muffle furnace at 600 °C for 2 h, which produced pure ZnO and Co:ZnO nanocrystals.

2.2. Characterization

The crystal structure of the samples was investigated using a Bruker-AXS D8 ADVANCE X-ray diffractometer (XRD) with Cu Kα radiation (λ = 0.15406 nm). FESEM

* Corresponding authors. Tel.: +86 311 86268342.
E-mail addresses: lipingchina@yahoo.com.cn (P. Li), weiyu@mail.hebtu.edu.cn (Y. Wei).

0925-8388/$ – see front matter © 2010 Elsevier B.V. All rights reserved.
doi:10.1016/j.jallcom.2010.05.183

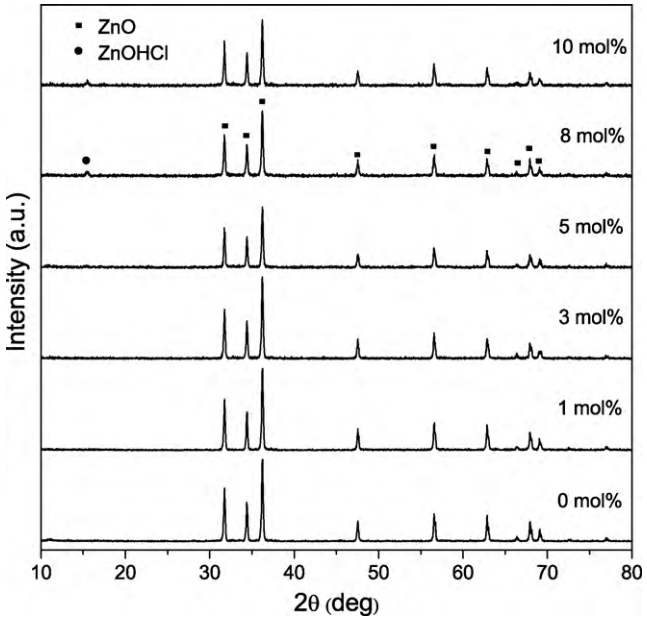

Fig. 1. XRD patterns obtained from ZnO nanocrystals doped with different levels of Co. The Co-doping levels are indicated alongside.

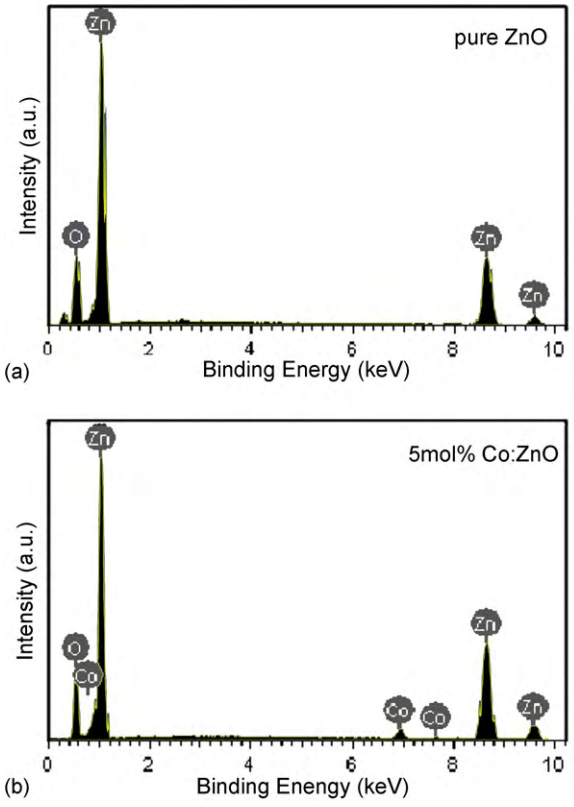

Fig. 2. EDS spectra of pure ZnO and 5 mol% Co:ZnO nanocrystals.

measurements were obtained on a HITACHI S-4800 field emission scanning electron microscopy. The dopant content after synthesis and the chemical bonding states of cobalt ions in the Co:ZnO nanocrystals were determined using EDS (OXFORD INCA ENERGY 350) and XPS (PHI-5702), respectively. Absorption spectra were collected with a SHIMADZU UV-2501PC UV–vis spectrophotometer. Photoluminescence (PL) spectra were collected at room temperature with a HITACHI F-4500 spectroscopy using Xe laser as an excitation source.

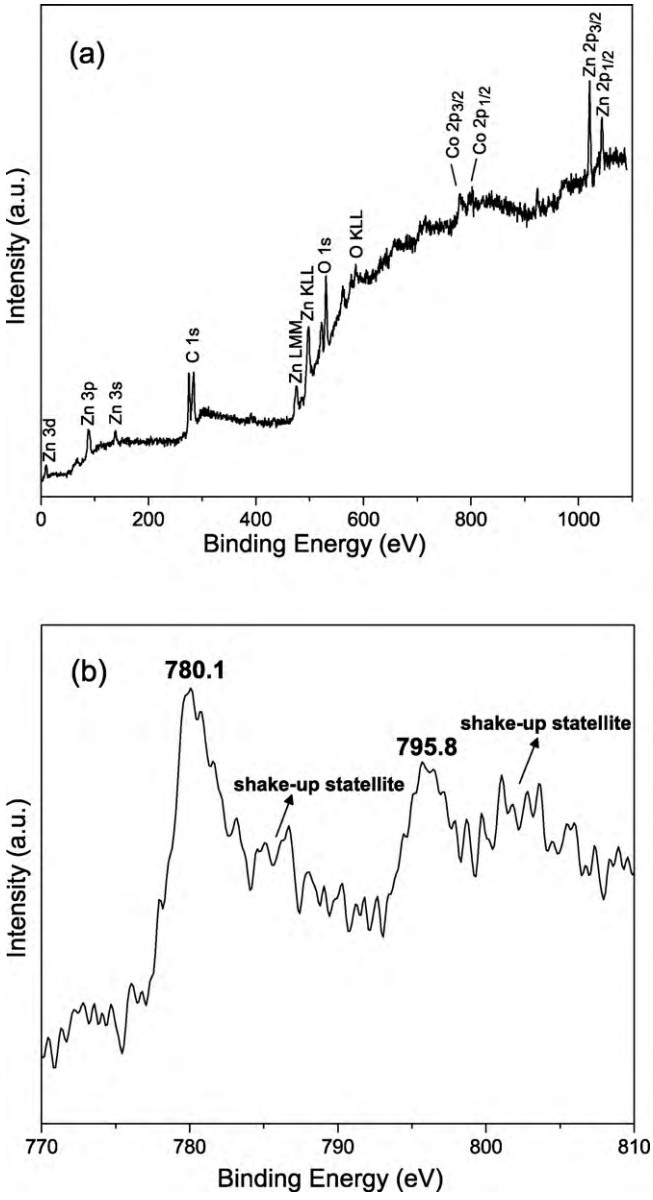

Fig. 3. (a) XPS spectrum of 8 mol% Co:ZnO nanocrystals. (b) High-resolution scan of Co $2p_{3/2}$ and $2p_{1/2}$ peaks.

3. Results and discussion

Compared with the white pure ZnO, the incorporation of Co is directly observed by the olive-green coloration of the Co:ZnO samples. Fig. 1 shows the XRD patterns of pure ZnO and Co:ZnO nanocrystals. The XRD patterns of the samples with 0–5 mol% doping levels reveal the presence of a single hexagonal phase with wurtzite structure (JCPDS No. 36-1451). The sharp and intense peaks indicate that all the samples are highly crystallized. Impurity phases such as metallic cobalt, cobalt oxides and other compounds cannot be detected. While the doping level is up to 8 mol%, trace of ZnOHCl begins to present in the Co:ZnO samples. It is well possible that the dopant atoms add a thermodynamical barrier to the phase transformation from the precursor precipitate to ZnO nanocrystals, resulting in a slowdown of the whole process. The calculated values of lattice parameters of the samples are listed in Table 1, using MDI Jade X-ray professional software. It can be found that the lattice parameters of *a*, *b* and *c* decrease slightly with the increasing Co content in the samples, inferring that part of Co ions with

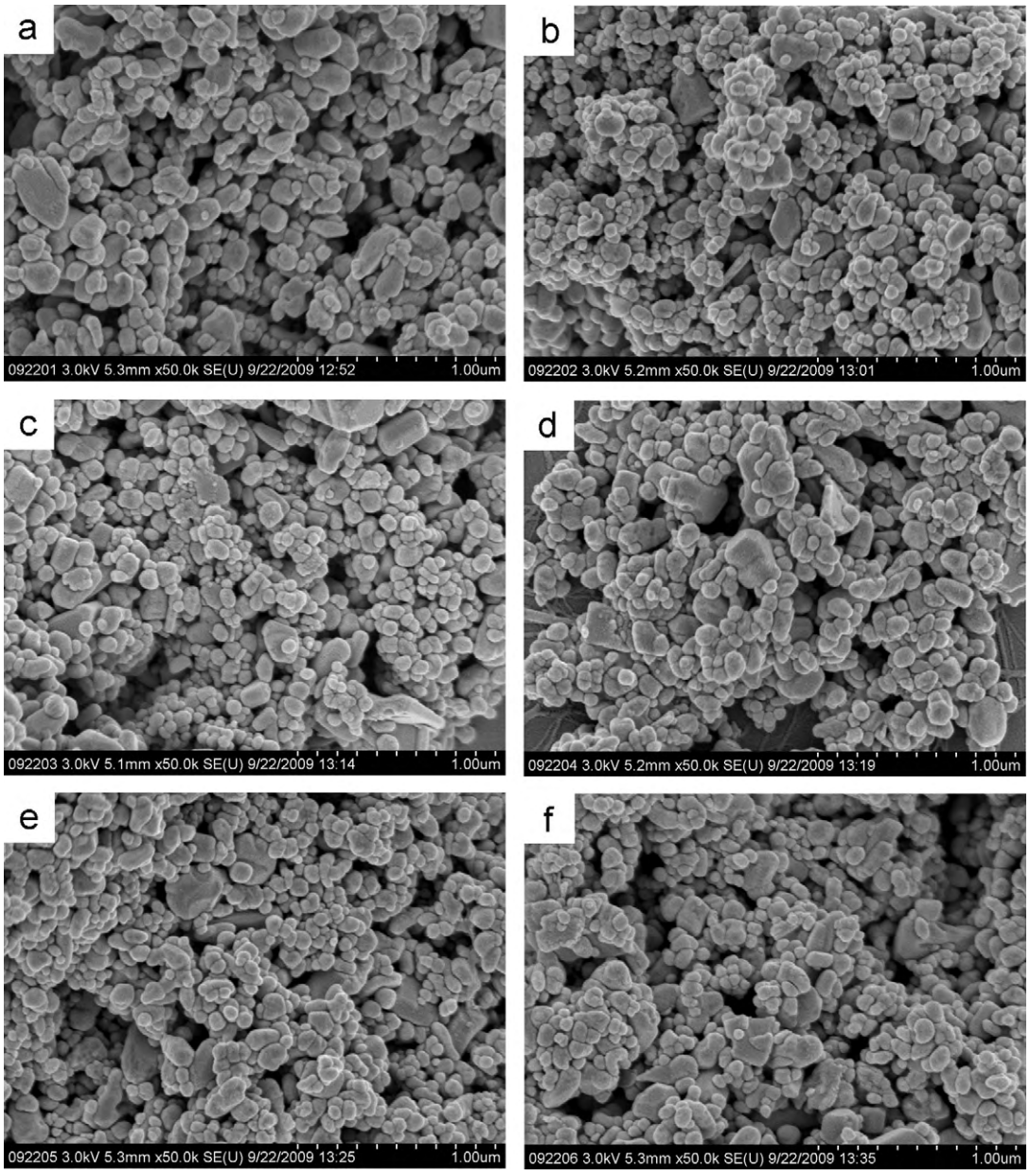

Fig. 4. FESEM images of ZnO nanocrystals doped with different levels of Co: (a) 0 mol%, (b) 1 mol%, (c) 3 mol%, (d) 5 mol%, (e) 8 mol% and (f) 10 mol%.

small ionic radii replace Zn ions in the ZnO lattice without changing the wurtzite structure. In addition, Co ions introduced as dopants at levels 1–10 mol% shift the diffraction peaks to higher angles (0.02–0.06°), compared to pure ZnO. Such a change also suggests that Co ions replace Zn ions in the lattice and the unit cell contracts to accommodate the heterogeneous ions, because Co ions have smaller ionic radii than Zn ions.

Fig. 2 shows the energy-dispersive spectra (EDS) of pure ZnO and 5 mol% Co:ZnO nanocrystals. The spectra indicate the presence of Zn and O elements in pure ZnO and an additional Co element in the Co:ZnO sample. Semiquantitative analysis of the compositions shown in Table 2 reveals that the dopant content in the samples increases from 0.35 to 2.94 at.% depending on the Co-doping levels. In general, less Co is found in Co:ZnO crystals than provided in the precursor solution, indicating that part of the Co ions is remained in the solution rather than incorporated into the precipitate and then thrown away in the subsequent washing process.

Table 1
The calculated values of lattice parameters of ZnO nanocrystals with different Co-doping levels.

Co-doping levels (mol%)	Lattice parameter $a = b$ (Å)	Lattice parameter c (Å)
0	3.2342	5.1901
1	3.2336	5.1891
3	3.2273	5.1853
5	3.2253	5.1844

Table 2
The composition of ZnO nanocrystals dependence on Co-doping levels.

Composition (at.%)	Co-doping levels (mol%)					
	0	1	3	5	8	10
Zn	50.00	49.65	48.71	48.20	47.62	47.06
Co	0	0.35	1.29	1.80	2.38	2.94
O	50.00	50.00	50.00	50.00	50.00	50.00

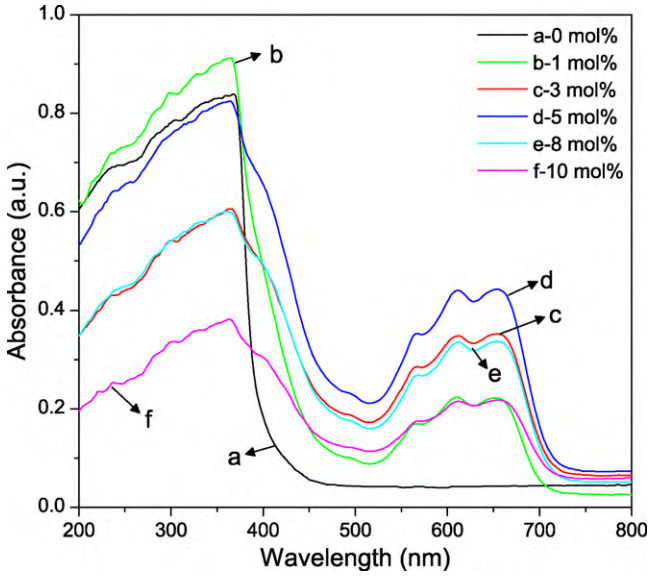

Fig. 5. UV–vis absorption spectra of ZnO nanocrystals doped with different levels of Co.

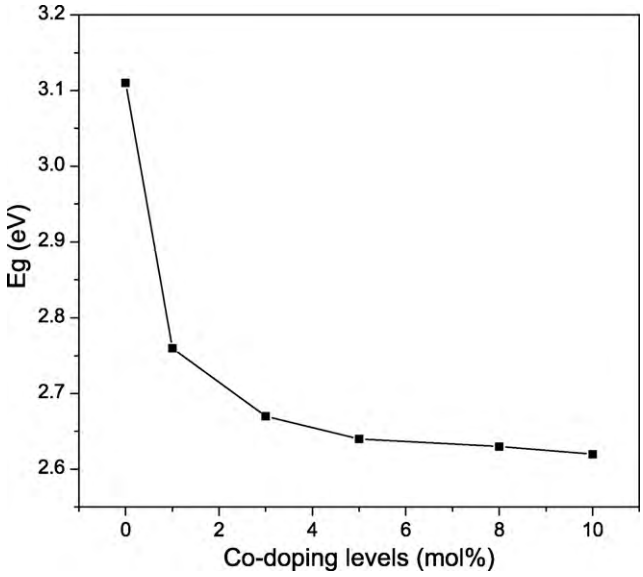

Fig. 6. Effect of Co-doping on the band gap of ZnO nanocrystals.

X-ray photoelectron spectroscopy (XPS) measurements were carried out to investigate the chemical bonding states of cobalt ions in the Co:ZnO nanocrystals. Fig. 3(a) shows the survey spectrum of the 8 mol% Co:ZnO sample. Two weak peaks are detected at the energy positions 775–800 eV, corresponding to Co $2p_{3/2}$ and Co $2p_{1/2}$ orbitals. Its slow scan in Fig. 3(b) shows Co $2p_{3/2}$ peaks at 780.1 eV and Co $2p_{1/2}$ at 795.8 eV. Also two shake-up satellites of the main peaks are present at slightly higher energies as indicated in Fig. 3(b). The satellite peak at ~786 eV is regarded as a feature of Co^{2+} ions [9]. Furthermore, the energy difference of 15.7 eV between Co $2p_{1/2}$ and Co $2p_{3/2}$ agrees with the literature data on Co^{2+} in CoO and Co:ZnO [27,28]. If the dopant exists as a single metal cluster in the Co:ZnO nanocrystals, then the energy difference should be 15.05 eV [29]. These facts confirm the 2+ oxidation state of the incorporated dopant. So we can conclude that the dopant atoms are well-incorporated in the host lattice as Co^{2+} on Zn lattice sites.

Field emission scanning electron microscopy (FESEM) can provide a direct observation of the morphology of nanomaterials. Fig. 4 shows the typical FESEM images of pure ZnO and Co:ZnO nanocrystals, revealing nearly spherical nanoparticles with moderate aggregation in most cases. The dimensions of the particles are in the range of 80–150 nm for pure ZnO and 50–120 nm for Co:ZnO. Obviously Co-doping has few significant effects on the morphology of the particles, but slightly reduces the particle size. It can be suggested that the aforementioned thermodynamical barrier induced by the dopant atoms causes a slowdown of the nanocrystals' growth. As a consequence, smaller particles are obtained.

UV–vis spectroscopies were carried out at room temperature to study the effect of Co-doping on the band gap of ZnO nanocrystals. Fig. 5 shows the typical absorption spectra of the samples doped with different levels of Co. An additional triplet peaks at approximately 570, 620 and 660 nm appear in the spectra of the Co-doped samples (from b to f) in comparison with pure ZnO. They are attributed to be $^4A_2(F) \rightarrow {}^2A_1(G)$, $^4A_2(F) \rightarrow {}^4T_1(P)$ and $^4A_2(F) \rightarrow {}^2E(G)$ transitions, suggesting the tetrahedrally coordinated Co^{2+} ions substituting for Zn^{2+} ions in the hexagonal ZnO wurtzite structure [30]. In addition, a large red shift of the absorption edges can be observed with the increasing Co-doping levels. The wavelength of the absorption edges was determined by extrapolation of the linear part to $A(\lambda) = 0$. Then we obtained the corresponding band gap energies of the samples, according to the formula $E = hc/\lambda$. Fig. 6 reveals that the band gap energy decreases from 3.11 to 2.62 eV with the increasing Co-doping levels, which might originate from the active transitions involving 3d levels in Co^{2+} ions and strong sp–d exchange interactions between the itinerant sp carriers (band electrons) and the localized d electrons of the dopant.

Photoluminescence (PL) is also a sensitive technique for measuring the band structure of a semiconductor. Fig. 7 shows the PL spectra of pure ZnO and Co:ZnO nanocrystals measured at room temperature. In general, the typical emission peaks in UV region are observed for all the samples, which can be assigned as a near-band-edge (NBE) emission band originating from the direct exciton recombination. However, no other visible emissions can be observed in the spectra, indicating that the samples prepared by this coprecipitation process are well-crystalline. There are few defect sites and singly ionized oxygen vacancies in the wurtzite lattice. Besides, it can be found that the UV emissions shift to the longer wavelength with the increasing Co-doping levels, as seen in pure ZnO with a maximum at about 378 nm and in 10 mol%

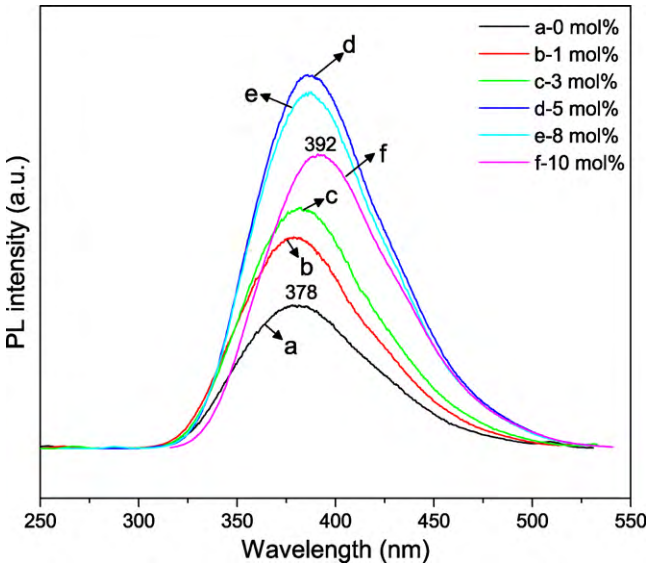

Fig. 7. PL spectra of ZnO nanocrystals doped with different levels of Co.

Co:ZnO at 392 nm. This is mainly due to the band gap narrowing of ZnO nanocrystals with the Co dopant, as discussed in the UV–vis absorption section. In addition, the intensity of the UV emissions is remarkably enhanced with 1–5 mol% doping levels, indicating that Co-doping can effectively improve the recombination of the free excitons in NBE. While the intensity of the emissions declines in 8 and 10 mol% Co:ZnO, which is owing to the existence of ZnOHCl impurity in the ZnO crystals acting as the non-radiative recombination centers for the electrons and holes.

4. Conclusions

Pure and Co-doped ZnO nanocrystals have been successfully synthesized by a simple coprecipitation process. It was found that cobalt ions, in the oxidation state of Co^{2+}, replace Zn^{2+} ions into the ZnO lattice without changing its wurtzite structure. The dopant content varies from 0.35 to 2.94% depending on Co-doping levels. Co-doping does not change the nearly spherical morphology of the crystals, but slightly reduces the particle size. Co-doping has a significant impact on the energy band structure of ZnO nanocrystals. The band gap decreases from 3.11 (pure ZnO) to 2.62 eV (10 mol% Co:ZnO) with the increasing Co-doping levels, which is responsible for the red shifts of the wavelength in UV absorption and PL emissions.

Acknowledgements

This work was supported by the grants from Natural Science Foundation of China (20877021), Key Programs of Science and Technology Research of Ministry of Education of China (210020), Key Projects in Applied Basic Research of Hebei Province (09963537D) and Hebei Normal University Funds (L2007B13 and L2008Z09).

References

[1] P.G. Li, W.H. Tang, X. Wang, J. Alloys Compd. 479 (2009) 634–637.
[2] L. Xu, Y. Su, Y.Q. Chen, H.H. Xiao, L.-A. Zhu, Q.T. Zhou, S. Li, J. Phys. Chem. B 110 (2006) 6637–6642.
[3] K. Iwata, H. Tampo, A. Yamada, P. Fons, K. Matsubara, K. Sakurai, S. Ishizuka, S. Niki, Appl. Surf. Sci. 244 (2005) 504–510.
[4] S.C. Zhang, X.G. Li, Colloids Surf. A 226 (2003) 35–44.
[5] P. Li, H. Liu, F.-X. Xu, Y. Wei, Mater. Chem. Phys. 112 (2008) 393–397.
[6] H.M. Yang, S. Nie, Mater. Chem. Phys. 114 (2009) 279–282.
[7] A.K. Singh, V. Viswanath, V.C. Janu, J. Lumin. 129 (2009) 874–878.
[8] Z. Zhang, J.B. Yi, J. Ding, L.M. Wong, H.L. Seng, S.J. Wang, J.G. Tao, G.P. Li, G.Z. Xing, T.C. Sum, C.H.A. Huan, T. Wu, J. Phys. Chem. C 112 (2008) 9579–9585.
[9] B.Q. Wang, C.H. Xia, J. Iqbal, N.J. Tang, Z.R. Sun, Y. Lv, L.N. Wu, Solid State Sci. 11 (2009) 1419–1422.
[10] X.Y. Zeng, J.L. Yuan, L.D. Zhang, J. Phys. Chem. C 112 (2008) 3503–3508.
[11] L. Armelao, G. Bottaro, M. Pascolini, M. Sessolo, E. Tondello, M. Bettinelli, A. Speghini, J. Phys. Chem. C 112 (2008) 4049–4054.
[12] J.H. Yang, Y. Cheng, Y. Liu, X. Ding, Y.X. Wang, Y.J. Zhang, H.L. Liu, Solid State Commun. 149 (2009) 1164–1167.
[13] Y.-J. Li, C.-Y. Wang, M.-Y. Lu, K.-M. Li, L.-J. Chen, Cryst. Growth Des. 8 (2008) 2598–2602.
[14] P. Lommens, F. Loncke, P.F. Smet, F. Callens, D. Poelman, H. Vrielinck, Z. Hens, Chem. Mater. 19 (2007) 5576–5583.
[15] T. Büsgen, M. Hilgendorff, S. Irsen, F. Wilhelm, A. Rogalev, D. Goll, M. Giersig, J. Phys. Chem. C 112 (2008) 2412–2417.
[16] M. Gaudon, O. Toulemonde, A. Demourgues, Inorg. Chem. 46 (2007) 10996–11002.
[17] X.Y. Zhou, S.H. Ge, D.S. Yao, Y.L. Zuo, Y.H. Xiao, J. Alloys Compd. 463 (2008) L9–L11.
[18] M.-Y. Choi, H.-K. Park, M.-J. Jin, D.H. Yoon, S.-W. Kim, J. Cryst. Growth 311 (2009) 504–507.
[19] N. Zhang, R. Yi, R.R. Shi, G.H. Gao, G. Chen, X.H. Liu, Mater. Lett. 63 (2009) 496–499.
[20] A. Khan, S.N. Khan, W.M. Jadwisienczak, M.E. Kordesch, Mater. Lett. 63 (2009) 2019–2021.
[21] S.J. Chen, G.R. Wang, Y.C. Liu, J. Lumin. 129 (2009) 340–343.
[22] C.C. Chen, P. Liu, C.H. Lu, Chem. Eng. J. 144 (2008) 509–513.
[23] P. Gao, Y.J. Chen, Y. Wang, Q. Zhang, X.F. Li, M. Hu, Chem. Commun. (2009) 2762–2764.
[24] B. Panigrahy, M. Aslam, D.S. Misra, D. Bahadur, CrystEngComm 11 (2009) 1920–1925.
[25] J.H. Yang, J.H. Zheng, H.J. Zhai, L.L. Yang, Y.J. Zhang, J.H. Lang, M. Gao, J. Alloys Compd. 475 (2009) 741–744.
[26] J.J. Qiu, X.M. Li, W.Z. He, S.-J. Park, H.-K. Kim, Y.-H. Hwang, J.-H. Lee, Y.-D. Kim, Nanotechnology 20 (2009) 155603.
[27] T.J. Chuang, C.R. Brundle, D.W. Rice, Surf. Sci. 59 (1976) 413–429.
[28] S. Deka, P.A. Joy, Solid State Commun. 134 (2005) 665–669.
[29] K.-C. Kim, E.-K. Kim, Y.-S. Kim, Superlattices Microstruct. 42 (2007) 246–250.
[30] H.A. Weakliem, J. Chem. Phys. 36 (1962) 2117–2141.